Identification of synergistic strategies for m^{6}A methylation-involved immunotherapy enhancement in lower grade gliomas

Qing Han (hanqing@email.ncu.edu.cn)
Nanchang University
Huimin He
Nanchang University

Research Article

Keywords: Lower grade gliomas, m6A, Immunotherapy, IL-6, macrophages

Posted Date: April 4th, 2022

DOI: https://doi.org/10.21203/rs.3.rs-1519458/v1

Abstract

Low grade gliomas (LGGs) are often noted for their unpredictable recurrence and transformation of malignancy to higher grade. Due to the extraordinary immunosuppressive microenvironment, LGGs seem to be refractory to T-cell based immunotherapies. Targeting RNA N6-methyladenosine (m^6A) modulated tumor microenvironment (TME) offers opportunities to trigger anti-LGG immunity. In our study, m^6Ascore were used for quantifying the m^6A modification patterns in LGGs. Potential therapeutic drugs and synergistic immunotherapy approaches which might avoid overtreatment and contribute to the TME remodeling were suggested based on the scoring scheme. We found a link between m^6Ascore and TME diversity. Those patients with high m^6Ascore and worse outcomes were more likely to experience immunotherapeutic failures. Inhibition of IL-6/JAK/STAT3 signaling that closely correlated with the drug sensitivities was indicated to facilitate the response of LGGs with high-m^6Ascore instead of overall LGGs to immune checkpoint blockade (ICB). Mechanically, stimulation of CD40 or TNFSF9 might reverse IL-6 inhibition induced insufficient activation of T cells by macrophages. In conclusion, synergistic immunotherapy of anti-IL-6 and ICB may offer insight into the m^6A related immunotherapy enhancement for LGG patients.

Introduction

Lower grade gliomas (LGGs), a sort of primary brain and CNS tumor, are taken to denote both World Health Organization grades II and III gliomas [1]. While some advances have been made in imaging [2] and treatment [3] of LGGs, the outcomes of the patients still remain unsatisfactory and a considerable proportion of them would experience the recurrence and transformation of malignancy to higher grade [4].

N6-methyladenosine, namely m^6A, is a modified base which has been known to present in ribosomal RNA, noncoding RNAs, polyadenylated RNA and mammalian mRNA [5]. To form m^6A methylation in mRNA accounts is considered to be the most abundant and vital mRNA internal modification which has emerged as an extensively gene expression-modulation mechanism in diverse physiological processes [6–8]. m^6A can be installed by methyltransferases termed "writers", removed by demethylases termed "erasers", and recognized by specific RNA-binding proteins termed "readers" [9]. Increasing evidences have demonstrated the crucial impacts of m^6A methylation modification on the maintenance of tumor cell stemness [10], DNA damage response [11], metastasis [12] and drug resistance [13], *et al*. Nevertheless, the roles of m^6A RNA methylation in LGGs still remain unexplored.

Circumvent immune recognition is a hallmark of tumor [14]. It can occur through various mechanisms including tumor cell alterations that decrease immune recognition [15–17] and increase resistance to immunity cytotoxic effects [18, 19] as well as the establishment of the immunosuppressive microenvironment [20–22]. The significance of non-neoplastic stromal cells in the development of LGGs has been gradually recognized [23, 24]. Considering its extraordinary immunosuppressive microenvironment,

LGGs seem to be refractory to immunotherapies based on T cells including checkpoint inhibition and chimeric antigen receptor T cell transfer [25]. This highlights the urgent need to identify novel combination strategies to trigger anti-LGG immunity.

Present studies have revealed the effects of m^6A RNA methylation on TME modification [26–28]. Here, we systematically correlated the m^6A modification phenotypes with genomic and clinical characteristics of LGGs and established a novel scoring scheme to quantify the m^6A methylation modification patterns for individual LGG patients. Based on the scoring scheme, potential therapeutic drugs were prepared for TME remodeling related pathway analysis. We found that IL-6/JAK/STAT3 signaling inhibition had the potential to sensitize those patients with high m^6Ascore to immune checkpoint blockade (ICB), and suggested the stimulation of CD40 or TNFSF9 might reverse IL-6 inhibition induced insufficient activation of T cells by macrophages (Mϕs). Overall, our research provides possible strategies for overcoming the resistance to chemotherapy and immunotherapy under the specific m^6A modification pattern for LGG patients.

Material And Methods

Acquisition and processing of low grade glioma datasets

Public attainable expression profiles and the corresponding clinical annotation were obtained from the Cancer Genome Atlas (TCGA) database (https://cancergenome.nih.gov/), the Chinese Glioma Genome Atlas (CGGA) database (http://cgga.org.cn/) and Gene Expression Omnibus database (GSE151213). A total of 1040 LGG patients and mouse bone marrow-derived Mϕs treated with IL-6 were enrolled in the study, including those from TCGA-LGG cohort (n = 457), CCGA_mRNA_seq325 (n = 182), CGGA_mRNA_seq693 (n = 401) and GSE151213. Batch effects of raw data from CGGA were processed by the “sva” package. Then, FPKM values in data from TCGA, CGGA and GEO were transformed into transcripts per kilobase million (TPM) format for further analysis.

Phenotype Classification

Unsupervised clustering analysis was performed to identify m^6A methylation modification phenotypes based on the expression of 24 m^6A regulators and m^6A-modulated phenotypes based on the expression of perturbation genes through “ConsensuClusterPlus” package [29].

Functional annotation

To investigate the contrasts on biological process among m^6A methylation modification phenotypes, GSVA enrichment analysis [30] was utilized using “GSVA” packages. The hallmark gene sets were obtained from MSigDB database. Gene Ontology (GO) analysis on m^6A signature genes was performed via “clusterProfiler” package [31], which was also used to carry out “GSEA” analysis [32] to determine pathways

up- and downregulated between LGG-m^{6}Ascore high and low groups. Adjusted *p* values less than 0.05 were held to be statistically significant.

Exploration of gene expression perturbation among m6A phenotypes

To identify genes correlated with m^{6}A modification patterns, LGG patients were grouped into m^{6}A clusters. Differently expression genes (DEGs) among three clusters were determined using the "DEseq2" package [33]. The counts data of TCGA-LGG were downloaded from UCSC XENA (https://xenabrowser.net/). The significance criteria for gene filtering were set as log2FC > 1 while adjusted $p < 0.05$.

Tumor microenvironment estimation and immune response prediction

The infiltration abundance of each cell in the tumor microenvironment (TME) was quantified by ssGSEA algorithm. The gene sets marked immune cell types were achieved from the research of Charoentong[34]. CIBERSORT, a deconvolution algorithm was performed to infer cell type proportions in bulk tumor samples [35]. In addition, we used the ESTIMATE algorithm to predict immune and stromal cells infiltration and further infer tumor purity [36]. Finally, TIDE algorithm was utilized to quantify the tumor immune evasion patterns in tumor samples and predict immunotherapy benefits of each patient [37].

Generation of m^{6}A methylation modification signature

To quantify the m^{6}A modification patterns in individual samples, a scoring system termed m6Ascore was contrasted as following procedures:

The DEGs among different m^{6}A clusters were identified for the overlap gene extract. Then, the LGG patients were stratified for deeper analysis by the overlap DEGs using unsupervised clustering method. After that, principal component analysis (PCA) was constructed to generate m^{6}A modification signature. Both principal component 1 and component 2 were considered to serve as signature scores. The advantage of this method focuses the score on the largest block of well-correlated/ inverse-correlated genes in the set, while the contributions of genes which little track with other members were weighted down. Finally, we adopted a former formula to define the m6Ascore of each LGG patient [38, 39]: m6Ascore= $\sum$(PC1i + PC2i), where i is the gene expression in the signature.

Acquisition and processing of drug sensitivity data

Expression profile data from human cancer cell lines were obtained from the Broad Institute Cancer Cell Line Encyclopedia (CCLE) project (https://portals.broadinstitute.org/ccle/) for working as the training set. Drug sensitivity data was achieved from the Cancer Therapeutics Response Portal (CTRP) and Profiling Relative Inhibition Simultaneously in Mixtures (PRISM) dataset. Both two datasets provide AUC (the area under the curve) values as a drug sensitivity measure. Compounds with more than one fifth of missing

data were removed, while K nearest neighbor (k-NN) imputation was used for imputing the missing values. We identified the candidate compounds with different AUC values between LGG-m^{6}Ascore groups (log2FC > 0.1). Spearman correlation analysis was adopted to estimate the relationship between AUC value and m^{6}Ascore (Spearman's r < − 0.30).

Statistical analysis

R-4.0.2 was employed for statistical analyses. For quantified data, statistical significance between normally distributed variables was calculated by Student's t-tests, while that between non-normally distributed variables was checked by the Wilcoxon test. Chi-square test or Fisher exact test was used to exam correlation between two categorical variables. For survival analysis, Kaplan-Meier curves and the Cox proportional hazards models were performed by 'Survminer' package. The receiver operating characteristic (ROC) curves was utilized to verify the prognostic prediction performance via 'timeROC' package. Statistical significance was corresponded to *p* values: ns > 0.05, * <0.05, ** <0.01, *** <0.001.

Results

Construction of m6A methylation signatures in LGGs

The structural framework of this study was depicted **(**Fig. 1**).**To systematically investigate the m^{6}A modification patterns, a total of 24 m^{6}A regulators (the landscape of genetic alterations and prognostic analysis were shown in Figure S1) were enrolled for stratifying TCGA-LGG patients, among which IGF2BPs were significantly associated to the patients' prognosis (Fig. 2A, **Figure S2A-G**). Those patients with high immune infiltration were observed to have poor prognosis (Fig. 2B-D). Then, we tested known signatures to better describe the function of m^{6}A methylation modification in LGG, and confirmed its important regulatory roles in immune, stromal as well as mismatch repair (Fig. 2E). To learn more about the biological behaviors among the distinct m^{6}A modification phenotypes, GSVA analysis was performed. The phenotypes with poor prognosis related to pathways enriched in epithelial-mesenchymal transition, mismatch repair and cytokine-related pathway (Fig. 2F). After that, we used the ESTIMATE algorithm to assess the tumor purity levels which was significantly higher in Cluster C (Fig. 2G). CIBERSORT was also used to evaluate the fraction of TME cells among the m^{6}A clusters (Fig. 2H). In addition, LGGs with wild type IDH were mainly clustered into Cluster B&C, while IDH mutant samples were closely relevant to Cluster A (Fig. 2I). Finally, we determined 215 overlapping m^{6}A phenotype-related DEGs as the m^{6}A gene signature in LGGs (Fig. 2J).

To further investigate the clinical traits and potential biological behavior of the m^{6}A modification signature, unsupervised clustering analyses was performed to identify three typical subtypes termed 'Gene cluster' (Fig. 3A). Overall survival analysis and progression free survival analysis revealed that patients in gene cluster B experienced the outcomes of poor prognosis (Fig. 3B-C). 24 m^{6}A regulators involved in this study showed significant expression perturbations among the three gene clusters (Fig. 3D). A significant higher infraction level of TME cells and elevated expression level of immune-

checkpoints were indicated in the gene cluster B (Fig. 3E-F). In addition, we also evaluated the enrichment of mismatch repair and stromal relevant signatures which were remarkably difference among the three gene clusters (Fig. 3G). Furthermore, functional annotations on the genes in the m^{6}A gene signature were carried out. The results showed that the m6A-related genes were widely involved in the maintenance of tumor stemness, radiotherapy, proliferation and metabolism and immunity (Fig. 3H).

Quantifying the m6A methylation modification in an independent individual

To quantifying the m^{6}A methylation modification in an independent individual, we generated a scoring scheme termed “m^{6}Ascore” based on the m^{6}A signature via the PCA algorithm. The attribute changes of LGG patients were illustrated by an alluvial diagram (Fig. 4A). m^{6}Ascore was positively correlated with the expression levels of CD8$^+$ T effectors and immune checkpoints (Fig. 4B), which suggested the pre-existence of immune response in the tumors with high m^{6}Ascore and then followed by T-cell exhaustion. Moreover, the m^{6}Ascore was markedly positively correlated with EMT signatures but negatively correlated with stromal relevant signatures. The results of GSEA revealed the differentially enriched pathways between the m^{6}Ascore groups, such as “MAPK cascade”, “ERK1/2 cascades” and “JAK/STAT signaling” (Fig. 4C). After that, we analyzed the somatic mutation differences between high- and low-m^{6}Ascore groups in TCGA-LGG cohort (Fig. 4D). The genes with significantly different distributions among the genes with TOP10 mutant frequency in the TCGA-LGG patients were shown in Figure S5. Then, we analyzed the clinical and molecular features between the LGG-m^{6}Ascore groups. The significant distinct distributions of primary location, grade, age and molecular subtypes were observed between the m^{6}Ascore groups. Patients with high m^{6}score were remarkably associated with worse prognosis (Fig. 4F-H). What’s more, an increasing number of studies have revealed the significant roles of TME in the development of LGGs [40] and the feasibility of immunotherapy in brain tumors [41, 42]. We assessed the benefit of immune checkpoint blockage (ICB) therapy. Those patients with high m^{6}Ascore and worse prognosis also predicted to benefit less from ICB therapy (Fig. 4I-J). Thus, it is urgent for LGG patients to identify ICB sensitization strategies.

Identification of the key m^{6}A relevant signaling pathway for immunotherapy enhancement

Instead of merely analyzing gene expression perturbation, we expected to obtain the sensitive drug compounds applied in high-m^{6}Ascore LGGs for TME remodeling as well as their associated pathways which might contribute to ICB sensitization. We first identified drug candidates with greater sensitivity to high LGG-m^{6}Ascore patients [43]. The analyses were based on the drug response data of CTRP [44–46] and PRISM, including 1,639 compounds. Totally 16 compounds were yielded with higher sensitivity by the analysis, while the most widespread chemotherapy for glioma patients, temozolomide, was detected to had lower sensitivity in high m^{6}Ascore patients (Fig. 5A-C). Afterwards, correlation analysis was adopted

to select TAK-733, clofarabine, dasatinib and birinapant as the optimal therapeutic agents to those LGGs the immune suppressed microenvironment (Fig. 5D-E). It was found that the sensitivities of LGGs to these four candidates were all positively correlated with the enrichment of IL-6/JAK/STAT3 signaling (Fig. 5F). Together, our data revealed that IL-6/JAK/STAT3 might be a potential therapeutic targeting to trigger anti-LGG immunity to avoid ineffective overtreatment.

Inhibition of IL-6/JAK/STAT3 signaling sensitized LGGs with high m^6Ascore to immune checkpoint blockade

We first evaluated the relationship between IL-6/JAK/STAT3 signaling activation and prognosis. Higher enrichment of IL-6/JAK/STAT3 signaling was associated with the worse prognosis (Fig. 6A-B). Assessing the ICB treatment benefits, however, we did not observe less enrichment of IL-6/JAK/STAT3 signaling in the ICB-benefit group compared with non-benefit group in overall patients (Fig. 6C). Therefore, we stratified TCGA-LGG patients. It was found that IL-6/JAK/STAT3 signaling was lower enriched in the predicted ICB-beneficial patients with the high LGG-m^6Ascore, while this pathway was significantly enriched in ICB-beneficial patients with median and low m^6Ascore (Fig. 6D). Similarly, highly enriched IL-6/JAK/STAT3 signaling associated with poor outcomes (Fig. 6E) was observed in ICB non-benefit LGGs with high m^6Ascore, while there was no significant difference in the overall CGGA-LGG patients (Fig. 6F-G). Tumor-associated Mϕs have a pivotal role in cancer immunosuppression and therapy resistance [24, 47, 48]. We first evaluated the infiltration level and polarization of Mϕs in different m^6Ascore groups. We found that high-m^6Ascore group had an equal level of M2 macrophages and higher level of M0 and M1 macrophages compared with the other groups, albeit, the expression level of IL-6 which contributed to the macrophage infiltration and polarization was higher in high-m^6Ascore group (Fig. 6H-I). IL-6 neutralization has been proved to moderately enhance infiltration of $CD3^+$ $CD8^+$T cells into the tumors but do not activate these T cells, and reduced recruitment of $CD45^+CD11b^+F4/80^+$ Mϕs [49]. We therefore speculated that IL-6 neutralization might lead to insufficient activation of T cells by Mϕs, and perhaps there are certain mechanisms in protecting IL-6 downstream from IL-6 inhibition in the patients with high m^6Ascore.

RNA-seq data revealed that IL-6 could stimulate the expression of the members of tumor necrosis factor (TNF) superfamilies (cd40, tnfsf4, tnfsf9, tnfsf14, tnfsf15) in mouse bone marrow-derived Mϕs (Fig. 6J-L). We ranked TCGA and CGGA samples according to their IL-6 expression levels from low to high, selected the LGGs with the lowest IL-6 expression, and ensured that there was no significant difference in IL-6 expression levels between the m^6Ascore groups (Fig. 6M). We were surprised to find that CD40 and TNFSF9 expression were dramatically higher in high-m^6Ascore group than in other groups (Fig. 6N-R).

In conclusion, our study built a m^6A scoring scheme, based on which synergistic immunotherapy of IL-6 neutralization and ICB might be considered as an effective therapeutic strategy for LGGs with high

m^{6}Ascore, for the stimulation of CD40 or TNFSF9 might reverse IL-6 inhibition induced insufficient activation of T cells by Mϕs.

Discussion

Tumor associated T cell actication by ICB is one of the most successful approaches for cancer immunotherapy and expected to improve the prognosis of LGG patients. However, it is poorly studied in LGGs. Recently, growing efforts have focused on the m^{6}A RNA methylation and it's impacts on cancer immune editing [50]. Here, we developed the m^{6}Ascore to quantify the m^{6}A methylation modification patterns in individuals and a dual-targeted strategy including anti-IL-6 and ICB to reverse T cell exhaustion for those patients with high-m^{6}Ascore LGGs.

Based on the existing evidence of m^{6}A methylation modification network, 24 m^{6}A regulators were involved in the study and stratified the the tumor samples. DEGs among the distinct m^{6}A phenotypes were identified and considered as a m^{6}A relevant signature in LGG, which was a biomarker designed to classify m^{6}A modification patterns. The expressions of m^{6}A regulators in gene cluster B were significantly higher than in the other two clusters, and the expressions of immune-checkpoints and gatheration of suppressive cells in gene cluster A&C were remarkably decreased. Patients in gene cluster B experienced the worst clinical outcomes.Then, we constructed a scoring scheme termed 'm^{6}Ascore' to quantify the m^{6}A methylation modification patterns which can act as an indipendent prognostic biomarker for LGG patients. In addition, the results of our analyses showed the correlation between m^{6}Ascore with the genomic aberrations, especialy with IDH1, EGFR and TP53 mutation status. Then, we determined whether m^{6}Ascore can predict immunotherapy benefit in LGG. It is observed that there were less predicted ICB benefits in m^{6}Ascore-high group compared with m^{6}Ascore-low group. Thus, we expected to explore potential strategies to make those non-benefit patients benefit from immunotherapy.

IL-6, a pleiotropic cytokine, was recognized as a key cytokine to promote inflammation at first [51]. Recent studies has suggested that IL-6/JAK/STAT3 inhibited functional maturation of DC and suppressed effector T cells which blocked anti-tumor immunity [52]. IL-6 promoted M2 Mϕs polarization [53, 54] and tumors with high IL-6 expression with infiltration of PD1$^+$CD8$^+$ T cells and M2 Mϕs predicted poor prognosis [55]. In our study, we used cell line expression profiles and their drug sensitivity results to predict the sensitive drugs of TCGA-LGG with high m^{6}Ascore by machine learning, and found the key pathway, IL6/JAK/STAT3, related to TME modulation. However, anti-IL-6 therapy showed the modest efficacy to synergize with ICB out of the patients with high ower m^{6}Ascore LGGs, suggesting that there are certain mechanisms to protect the downstreams of IL-6 from anti-IL-6 therapy.

Multiple studies have revealed the significant impacts of TNF superfamily on macrophage activation and their co-stimulation of T cells to promote anti-tumor immunity [56, 57]. Thus, we analyzed the expression profile of Mϕs treated with IL-6, and found that IL-6 significantly up-regulated the expression of cd40, tnfsf4, tnfsf9, tnfsf14 and tnfsf15. Then, we found that the expression level of CD40 and TNFSF9 was

significantly higher in m6Ascore-high group than the other groups when the expression of IL-6 remained same low level at different m^6Ascore groups. These results illustrate a phynomenon that anti-IL-6 monotherapy might not fully reverse macrophage-mediated immunosuppression. Dual-targeting of CD40/TNFSF9 and IL-6 might cooperate immunotherapy of LGGs.

In summary, our study established the m^6Ascore to quantifying the m^6A methylation modification in individuals. For LGG patients with high m^6Ascores, we found some therapeutic drugs to avoid overtreatment and chemotherapy resistance. In the meanwhile, our findings suggested that dual-targeted stratergy including anti-IL-6 and ICB might trigger anti-tumor immunity for the patients with high-m^6Ascore LGGs which offered opportunities for facilitating T-cell based immunotherapy against LGGs.

Declarations

Ethical Approval and Consent to participate

The patient data involved in this study were acquired from publicly available datasets with the patients' informed consent.

Consent for publication

All authors have read and approved the final submitted manuscript.

Availability of supporting data

Public attainable expression profiles and the corresponding clinical annotation can be obtained from the Cancer Genome Atlas (TCGA) database (https://cancergenome.nih.gov/) and the Chinese Glioma Genome Atlas (CGGA) database (http://cgga.org.cn/). Methods used for the analyses and all generated results in this study are described in the supplementary data.

Competing interests

No potential conflicts of interest were disclosed.

Authors' contributions

Q. H. designed the study. Q. H. and HM. H. collated the data, carried out data analyses and produced the initial draft of the manuscript. Q. H. contributed to drafting the manuscript.

Acknowledgments

We would like to appreciate Dr. Zewei Tu for the crucial advice on this study.

References

1. Cancer Genome Atlas Research, N, Brat, DJ, Verhaak, RG, Aldape, KD, Yung, WK, Salama, SR, *et al.*Comprehensive, Integrative Genomic Analysis of Diffuse Lower-Grade Gliomas.N Engl J Med.2015;372:2481–2498
2. Zhou, H, Vallieres, M, Bai, HX, Su, C, Tang, H, Oldridge, D, *et al.*MRI features predict survival and molecular markers in diffuse lower-grade gliomas.Neuro Oncol.2017;19:862–870
3. Morshed, RA, Young, JS, Hervey-Jumper, SL, and Berger, MS.The management of low-grade gliomas in adults.J Neurosurg Sci.2019;63:450–457
4. Jaeckle, KA, Decker, PA, Ballman, KV, Flynn, PJ, Giannini, C, Scheithauer, BW, *et al.*Transformation of low grade glioma and correlation with outcome: an NCCTG database analysis.J Neurooncol.2011;104:253–259
5. Meyer, KD, and Jaffrey, SR.The dynamic epitranscriptome: N6-methyladenosine and gene expression control.Nat Rev Mol Cell Biol.2014;15:313–326
6. Zaccara, S, Ries, RJ, and Jaffrey, SR.Reading, writing and erasing mRNA methylation.Nat Rev Mol Cell Biol.2019;20:608–624
7. Sun, T, Wu, R, and Ming, L.The role of m6A RNA methylation in cancer.Biomed Pharmacother.2019;112:108613
8. Wang, T, Kong, S, Tao, M, and Ju, S.The potential role of RNA N6-methyladenosine in Cancer progression.Mol Cancer.2020;19:88
9. Chen, XY, Zhang, J, and Zhu, JS.The role of m(6)A RNA methylation in human cancer.Mol Cancer.2019;18:103
10. Zhang, S, Zhao, BS, Zhou, A, Lin, K, Zheng, S, Lu, Z, *et al.*m(6)A Demethylase ALKBH5 Maintains Tumorigenicity of Glioblastoma Stem-like Cells by Sustaining FOXM1 Expression and Cell Proliferation Program.Cancer Cell.2017;31:591–606 e596
11. Miranda-Goncalves, V, Lobo, J, Guimaraes-Teixeira, C, Barros-Silva, D, Guimaraes, R, Cantante, M, *et al.*The component of the m(6)A writer complex VIRMA is implicated in aggressive tumor phenotype, DNA damage response and cisplatin resistance in germ cell tumors.J Exp Clin Cancer Res.2021;40:268
12. Chang, G, Shi, L, Ye, Y, Shi, H, Zeng, L, Tiwary, S, *et al.*YTHDF3 Induces the Translation of m(6)A-Enriched Gene Transcripts to Promote Breast Cancer Brain Metastasis.Cancer Cell.2020;38:857–871 e857
13. Lan, Q, Liu, PY, Bell, JL, Wang, JY, Huttelmaier, S, Zhang, XD, *et al.*The Emerging Roles of RNA m(6)A Methylation and Demethylation as Critical Regulators of Tumorigenesis, Drug Sensitivity, and Resistance.Cancer Res.2021;81:3431–3440
14. Schreiber, RD, Old, LJ, and Smyth, MJ.Cancer immunoediting: integrating immunity's roles in cancer suppression and promotion.Science.2011;331:1565–1570
15. Chowell, D, Morris, LGT, Grigg, CM, Weber, JK, Samstein, RM, Makarov, V, *et al.*Patient HLA class I genotype influences cancer response to checkpoint blockade immunotherapy.Science.2018;359:582–587

16. Gettinger, S, Choi, J, Hastings, K, Truini, A, Datar, I, Sowell, R, *et al.*Impaired HLA Class I Antigen Processing and Presentation as a Mechanism of Acquired Resistance to Immune Checkpoint Inhibitors in Lung Cancer.Cancer Discov.2017;7:1420–1435
17. Restifo, NP, Marincola, FM, Kawakami, Y, Taubenberger, J, Yannelli, JR, and Rosenberg, SA.Loss of functional beta 2-microglobulin in metastatic melanomas from five patients receiving immunotherapy.J Natl Cancer Inst.1996;88:100–108
18. Sade-Feldman, M, Jiao, YJ, Chen, JH, Rooney, MS, Barzily-Rokni, M, Eliane, JP, *et al.*Resistance to checkpoint blockade therapy through inactivation of antigen presentation.Nat Commun.2017;8:1136
19. Zaretsky, JM, Garcia-Diaz, A, Shin, DS, Escuin-Ordinas, H, Hugo, W, Hu-Lieskovan, S, *et al.*Mutations Associated with Acquired Resistance to PD-1 Blockade in Melanoma.N Engl J Med.2016;375:819–829
20. Nakamura, K, and Smyth, MJ.Myeloid immunosuppression and immune checkpoints in the tumor microenvironment.Cell Mol Immunol.2020;17:1–12
21. Hofer, F, Di Sario, G, Musiu, C, Sartoris, S, De Sanctis, F, and Ugel, S.A Complex Metabolic Network Confers Immunosuppressive Functions to Myeloid-Derived Suppressor Cells (MDSCs) within the Tumour Microenvironment.Cells.2021;10:
22. Wherry, EJ.T cell exhaustion.Nat Immunol.2011;12:492–499
23. Wu, F, Wang, ZL, Wang, KY, Li, GZ, Chai, RC, Liu, YQ, *et al.*Classification of diffuse lower-grade glioma based on immunological profiling.Mol Oncol.2020;14:2081–2095
24. Grabowski, MM, Sankey, EW, Ryan, KJ, Chongsathidkiet, P, Lorrey, SJ, Wilkinson, DS, *et al.*Immune suppression in gliomas.J Neurooncol.2021;151:3–12
25. Haddad, AF, Young, JS, Oh, JY, Okada, H, and Aghi, MK.The immunology of low-grade gliomas.Neurosurg Focus.2022;52:E2
26. Li, HB, Tong, J, Zhu, S, Batista, PJ, Duffy, EE, Zhao, J, *et al.*m(6)A mRNA methylation controls T cell homeostasis by targeting the IL-7/STAT5/SOCS pathways.Nature.2017;548:338–342
27. Li, M, Zha, X, and Wang, S.The role of N6-methyladenosine mRNA in the tumor microenvironment.Biochim Biophys Acta Rev Cancer.2021;1875:188522
28. Song, H, Song, J, Cheng, M, Zheng, M, Wang, T, Tian, S, *et al.*METTL3-mediated m(6)A RNA methylation promotes the anti-tumour immunity of natural killer cells.Nat Commun.2021;12:5522
29. Wilkerson, MD, and Hayes, DN.ConsensusClusterPlus: a class discovery tool with confidence assessments and item tracking.Bioinformatics.2010;26:1572–1573
30. Hanzelmann, S, Castelo, R, and Guinney, J.GSVA: gene set variation analysis for microarray and RNA-seq data.BMC Bioinformatics.2013;14:7
31. Yu, G, Wang, LG, Han, Y, and He, QY.clusterProfiler: an R package for comparing biological themes among gene clusters.OMICS.2012;16:284–287
32. Subramanian, A, Tamayo, P, Mootha, VK, Mukherjee, S, Ebert, BL, Gillette, MA, *et al.*Gene set enrichment analysis: a knowledge-based approach for interpreting genome-wide expression

profiles.Proc Natl Acad Sci U S A.2005;102:15545–15550

33. Love, MI, Huber, W, and Anders, S.Moderated estimation of fold change and dispersion for RNA-seq data with DESeq2.Genome Biol.2014;15:550
34. Charoentong, P, Finotello, F, Angelova, M, Mayer, C, Efremova, M, Rieder, D, *et al.*Pan-cancer Immunogenomic Analyses Reveal Genotype-Immunophenotype Relationships and Predictors of Response to Checkpoint Blockade.Cell Rep.2017;18:248–262
35. Newman, AM, Liu, CL, Green, MR, Gentles, AJ, Feng, W, Xu, Y, *et al.*Robust enumeration of cell subsets from tissue expression profiles.Nat Methods.2015;12:453–457
36. Yoshihara, K, Shahmoradgoli, M, Martinez, E, Vegesna, R, Kim, H, Torres-Garcia, W, *et al.*Inferring tumour purity and stromal and immune cell admixture from expression data.Nat Commun.2013;4:2612
37. Jiang, P, Gu, S, Pan, D, Fu, J, Sahu, A, Hu, X, *et al.*Signatures of T cell dysfunction and exclusion predict cancer immunotherapy response.Nat Med.2018;24:1550–1558
38. Zeng, D, Li, M, Zhou, R, Zhang, J, Sun, H, Shi, M, *et al.*Tumor Microenvironment Characterization in Gastric Cancer Identifies Prognostic and Immunotherapeutically Relevant Gene Signatures.Cancer Immunol Res.2019;7:737–750
39. Chong, W, Shang, L, Liu, J, Fang, Z, Du, F, Wu, H, *et al.*m(6)A regulator-based methylation modification patterns characterized by distinct tumor microenvironment immune profiles in colon cancer.Theranostics.2021;11:2201–2217
40. Klemm, F, Maas, RR, Bowman, RL, Kornete, M, Soukup, K, Nassiri, S, *et al.*Interrogation of the Microenvironmental Landscape in Brain Tumors Reveals Disease-Specific Alterations of Immune Cells.Cell.2020;181:1643–1660 e1617
41. Jin, L, Ge, H, Long, Y, Yang, C, Chang, YE, Mu, L, *et al.*CD70, a novel target of CAR T-cell therapy for gliomas.Neuro Oncol.2018;20:55–65
42. Gromeier, M, Brown, MC, Zhang, G, Lin, X, Chen, Y, Wei, Z, *et al.*Very low mutation burden is a feature of inflamed recurrent glioblastomas responsive to cancer immunotherapy.Nat Commun.2021;12:352
43. Yang, C, Huang, X, Li, Y, Chen, J, Lv, Y, and Dai, S.Prognosis and personalized treatment prediction in TP53-mutant hepatocellular carcinoma: an in silico strategy towards precision oncology.Brief Bioinform.2021;22:
44. Rees, MG, Seashore-Ludlow, B, Cheah, JH, Adams, DJ, Price, EV, Gill, S, *et al.*Correlating chemical sensitivity and basal gene expression reveals mechanism of action.Nat Chem Biol.2016;12:109–116
45. Seashore-Ludlow, B, Rees, MG, Cheah, JH, Cokol, M, Price, EV, Coletti, ME, *et al.*Harnessing Connectivity in a Large-Scale Small-Molecule Sensitivity Dataset.Cancer Discov.2015;5:1210–1223
46. Basu, A, Bodycombe, NE, Cheah, JH, Price, EV, Liu, K, Schaefer, GI, *et al.*An interactive resource to identify cancer genetic and lineage dependencies targeted by small molecules.Cell.2013;154:1151–1161

47. Quail, DF, and Joyce, JA.Microenvironmental regulation of tumor progression and metastasis.Nat Med.2013;19:1423–1437
48. Noy, R, and Pollard, JW.Tumor-associated macrophages: from mechanisms to therapy.Immunity.2014;41:49–61
49. Yang, F, He, Z, Duan, H, Zhang, D, Li, J, Yang, H, *et al.*Synergistic immunotherapy of glioblastoma by dual targeting of IL-6 and CD40.Nat Commun.2021;12:3424
50. Li, X, Ma, S, Deng, Y, Yi, P, and Yu, J.Targeting the RNA m(6)A modification for cancer immunotherapy.Mol Cancer.2022;21:76
51. Hunter, CA, and Jones, SA.IL-6 as a keystone cytokine in health and disease.Nat Immunol.2015;16:448–457
52. Kitamura, H, Ohno, Y, Toyoshima, Y, Ohtake, J, Homma, S, Kawamura, H, *et al.*Interleukin-6/STAT3 signaling as a promising target to improve the efficacy of cancer immunotherapy.Cancer Sci.2017;108:1947–1952
53. Weng, YS, Tseng, HY, Chen, YA, Shen, PC, Al Haq, AT, Chen, LM, *et al.*MCT-1/miR-34a/IL-6/IL-6R signaling axis promotes EMT progression, cancer stemness and M2 macrophage polarization in triple-negative breast cancer.Mol Cancer.2019;18:42
54. Yin, Z, Ma, T, Lin, Y, Lu, X, Zhang, C, Chen, S, *et al.*IL-6/STAT3 pathway intermediates M1/M2 macrophage polarization during the development of hepatocellular carcinoma.J Cell Biochem.2018;119:9419–9432
55. Kuo, IY, Yang, YE, Yang, PS, Tsai, YJ, Tzeng, HT, Cheng, HC, *et al.*Converged Rab37/IL-6 trafficking and STAT3/PD-1 transcription axes elicit an immunosuppressive lung tumor microenvironment.Theranostics.2021;11:7029–7044
56. So, T, and Ishii, N.The TNF-TNFR Family of Co-signal Molecules.Adv Exp Med Biol.2019;1189:53–84
57. Croft, M.The role of TNF superfamily members in T-cell function and diseases.Nat Rev Immunol.2009;9:271–285

Figures

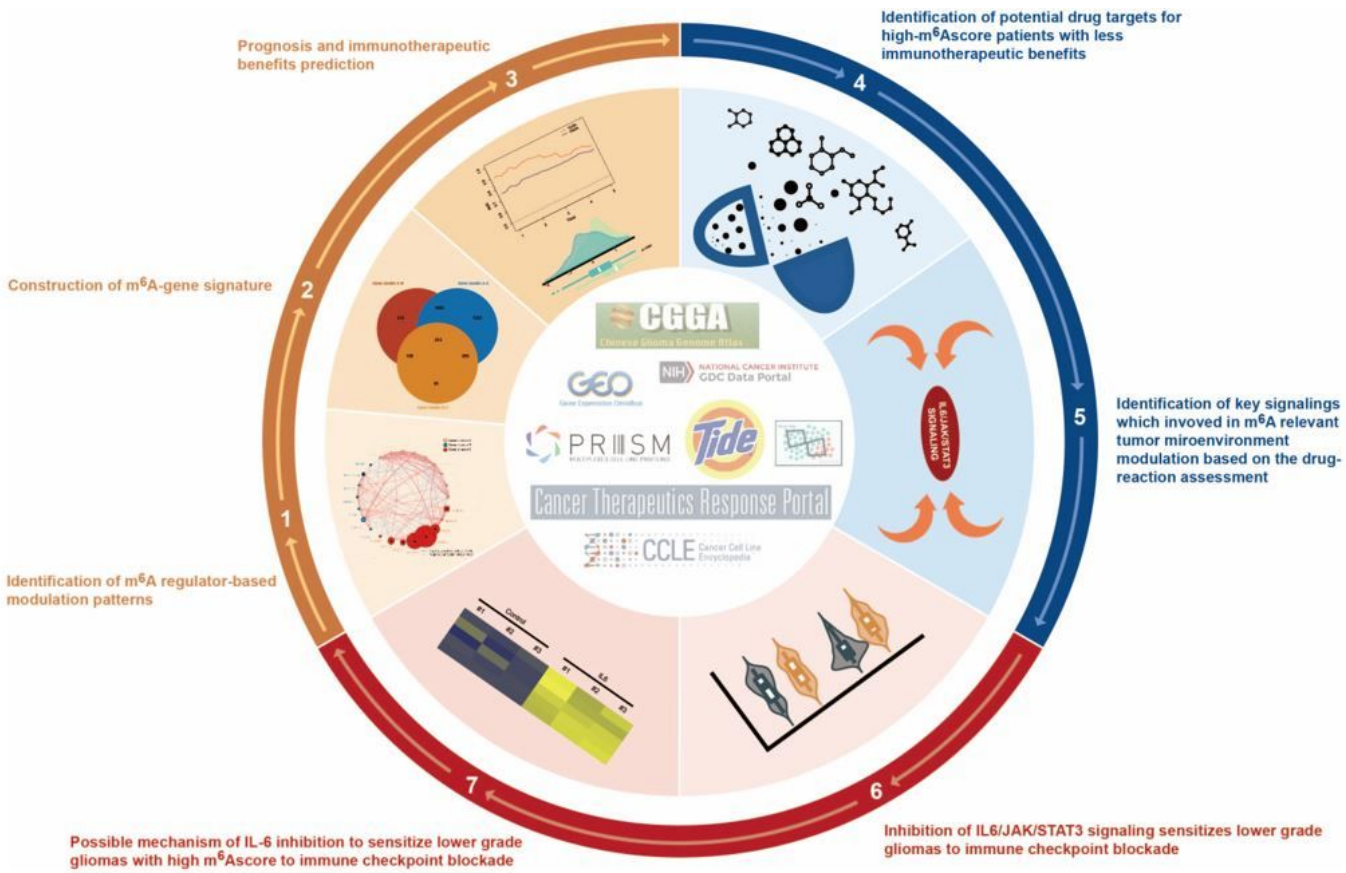

Figure 1

The structural framework of this study.

Figure 2

Construction of m^{6}A methylation signatures in LGGs. (A) Interactions between m^{6}A regulators in LGG. The size of circles represented the prognosis effect calculated by Log-rank test of the regulators. Green dot in each circles represented to be protective factors for overall survival, while black dot represented to be risk factors for overall survival. The lines linked with each other showed their interactions (blue for positivity; red for negativity), and thickness represented the correlation strength. (B) Heatmap of immune cell infractions in TCGA-LGG patients. Tumor purity, ESTIMATE score, immune score, stromal score, molecular subtype, age, gender and m^{6}A cluster were shown as annotations. (C) Overall survival analyses for the TCGA-LGG patients among the three m^{6}A-methylation modification patterns. (D) Progression free survival analyses for the TCGA-LGG patients among the three m^{6}A methylation modification patterns. (E) m^{6}A gene clusters were distinguished by different signatures. (F) GSVA enrichment analysis showed the difference on the biological behaviors among the m^{6}A methylation modification phenotypes. (G) Different levels of tumor purity in the distinct m^{6}A clusters. (H) TME cell fractions in the m^{6}A clusters calculated via the CIBERSORT algorithm. (I) Proportion of the LGG-molecular subtypes in the three m^{6}A

methylation modification patterns. (J) 215 m^6A phenotype-related DEGs among three m^6A clusters were shown by Venn diagram. Statistical significance was corresponded to *p* values: ns>0.05, * <0.05, ** <0.01, *** <0.001.

Figure 3

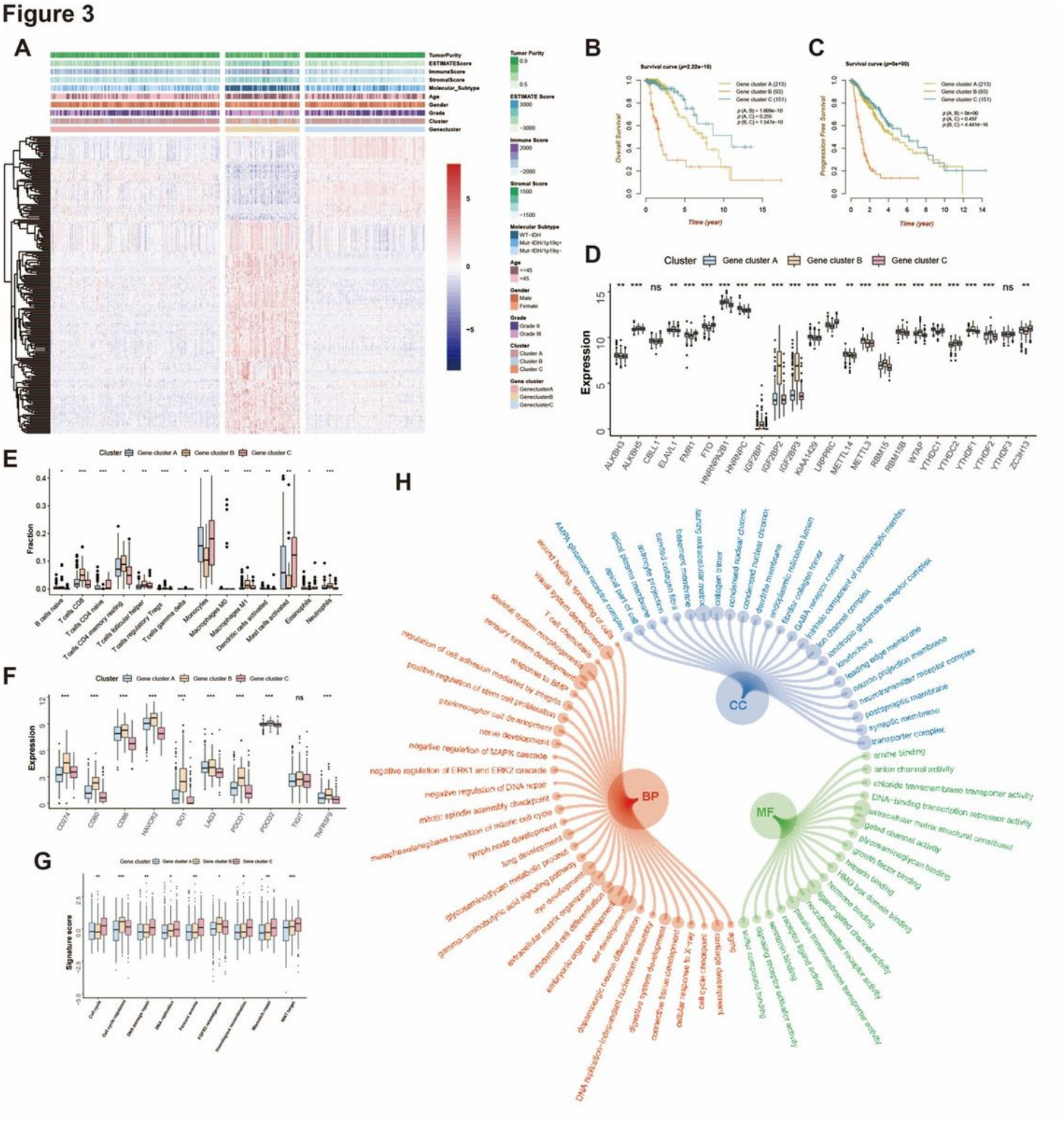

Figure 3

The functional annotation of the m^6A methylation signatures in LGG. (A) Unsupervised clustering of the m6A methylation modification relevant DEGs to stratify LGG patients into different genomic subtypes. (B) Overall survival analyses for the TCGA-LGG patients among the three m6A gene clusters. (C) Progression free survival analyses for the TCGA-LGG patients among the three m6A gene clusters. (D) Different expression levels of m^6A regulators among the m^6A gene clusters. (E) TME cell fractions in the m^6A clusters calculated via the CIBERSORT algorithm. (F) Different expression levels of immune-checkpoints among the m^6A gene clusters. (G) The m6A gene clusters were distinguished by different signatures. (H) Functional annotation for m6A phenotype relevant genes, adjusted *p* value <0.05. Statistical significance was corresponded to *p* values: ns>0.05, * <0.05, ** <0.01, *** <0.001.

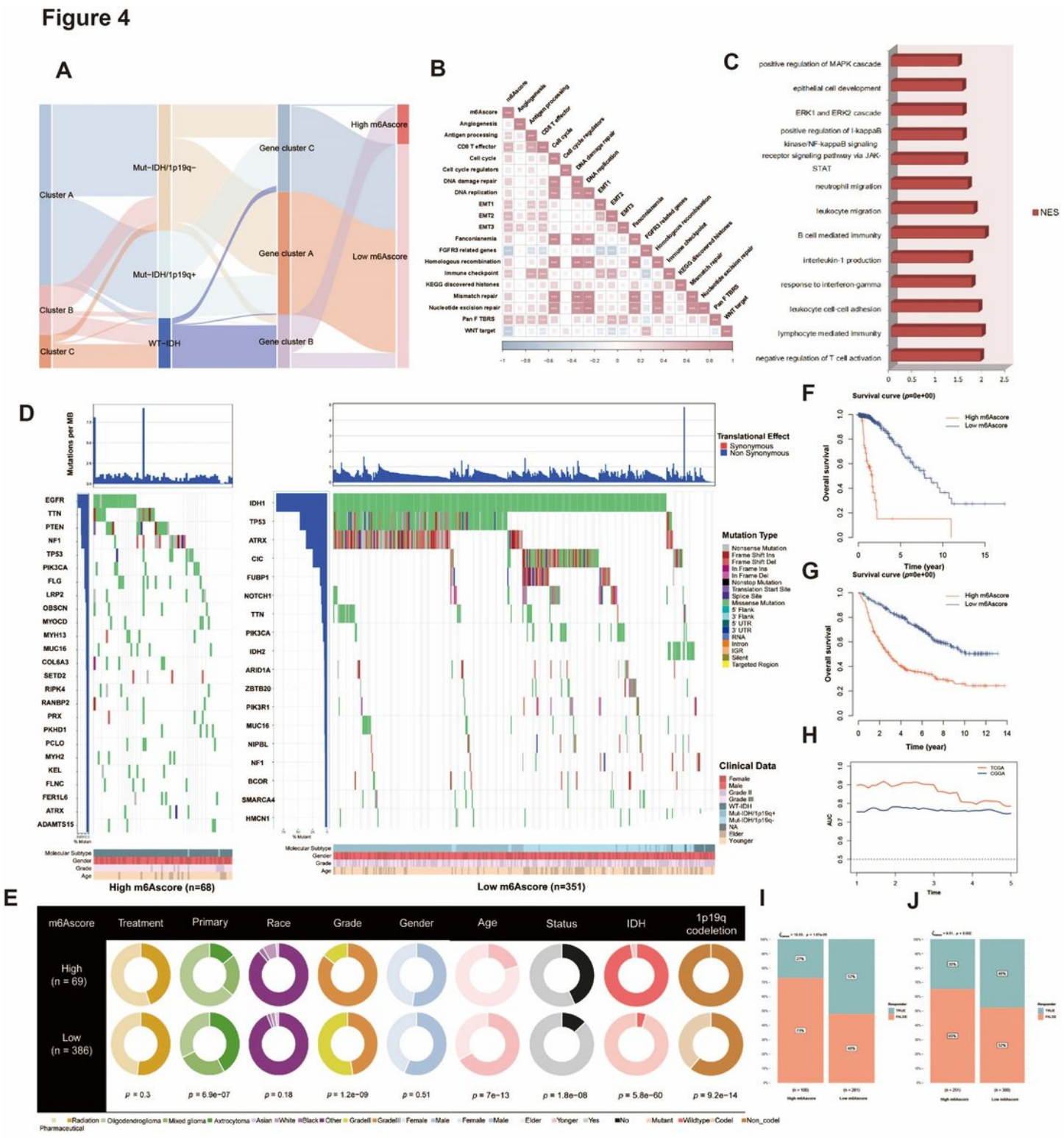

Figure 4

Quantifying the m^{6}A methylation modification in an independent individual. (A) Alluvial diagram showing the attribute changes of LGG patients in m^{6}A clusters, molecular subtypes, m^{6}A gene clusters and LGG-m^{6}Ascore. (B) Spearman analysis revealed the correlations between known signatures with LGG-m^{6}Ascore. (C) GSEA results of GO (biological process) gene sets between m^{6}Ascore-high and -low

groups, adjusted *p* value <0.05. (D) Mutational landscape of TCGA-LGG patients with high m^6Ascore on the left and low m^6Ascore on the right. The top bar plot indicates tumor mutation burden, while molecular subtype, age, gender and grade were shown as annotations on the bottom. (E) Clinical and molecular features between high- and low-m^6Ascore groups. (F) Overall survival analyses for LGG patients between low- and high-m^6Ascore groups in the TCGA cohort via Kaplan-Meier curves. (G) Overall survival analyses for LGG patients between low- and high-m^6Ascore groups in the meta-CGGA cohort via Kaplan-Meier curves. (H) The prognostic predictive effects of LGG-m^6Ascore in different cohorts were measured by ROC curves. (I) Predicted immunotherapy benefits via TIDE between high- and low-m^6Ascore groups in the TCGA cohort. (J) Predicted immunotherapy benefits via TIDE between high- and low-m^6Ascore groups in the meta-CGGA cohort.

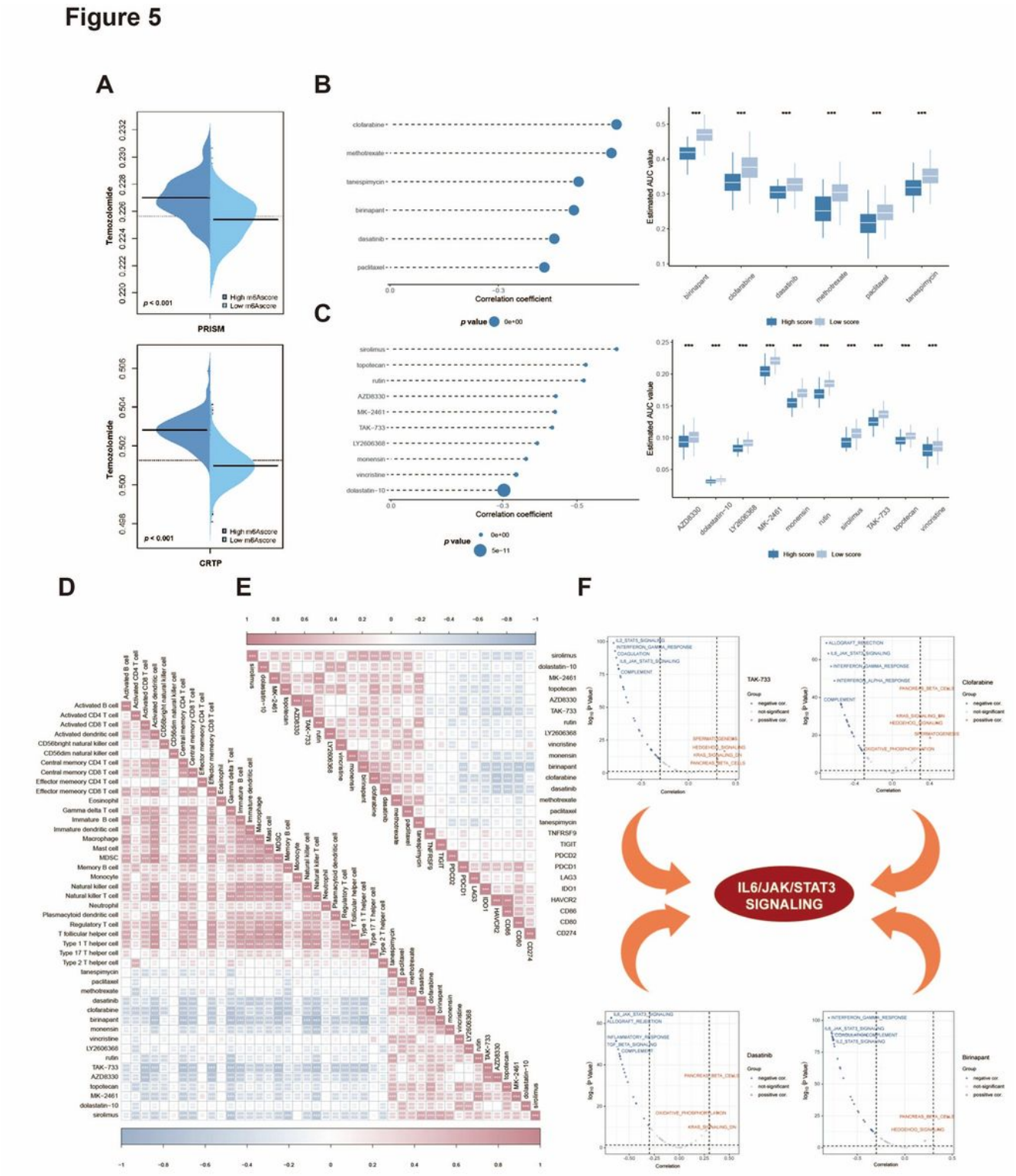

Figure 5

Identification of the key m^{6}A relevant signaling pathway for immunotherapy enhancement. (A) The sensitivity of LGG patients to TMZ treatment between m^{6}Ascore-high and -low groups was calculated based on PRISM and CRTP database. (B-C) Spearman's correlation and drug response of CTRP-derived compounds on the top and PRISM-derived compounds on the bottom. Compounds with lower AUC value in m^{6}Ascore-high group and negative closely correlated with m^{6}Ascore were selected as potential

therapeutic drugs. Lower values of AUC indicated greater drug sensitivity. (D) Correlation between drug sensitivities of potential therapeutic agents and immune cell infiltrations. (E) Correlation between drug sensitivities of potential therapeutic agents and expression levels of immune checkpoints. (F) Correlation between drug sensitivities of potential therapeutic agents and enrichment of signaling pathways. Statistical significance was corresponded to *p* values: ns>0.05, * <0.05, ** <0.01, *** <0.001.

Figure 6

Inhibition of IL-6/JAK/STAT3 signaling sensitized lower grade gliomas to immune checkpoint blockade. Overall survival analyses (A) and progression free survival analyses (B) for the TCGA-LGG patients between high- and low- enrichment of IL-6/JAK/STAT3 signaling via Kaplan-Meier curves. (C) Relative distribution of IL-6/JAK/STAT3 signaling enrichment score between TURE and FALSE response of TIDE in the overall TCGA-LLG patients. (D) Relative distribution of IL-6/JAK/STAT3 signaling enrichment score between TURE and FALSE response at different LGG-m^6Ascore levels. (E) Overall survival analyses for the CGGA-LGG patients between high- and low- enrichment of IL-6/JAK/STAT3 signaling via Kaplan-Meier curves. (F) Relative distribution of IL-6/JAK/STAT3 signaling enrichment score between TURE and FALSE response in overall CGGA-LGG patients. (G) Relative distribution of IL-6/JAK/STAT3 signaling enrichment score between TURE and FALSE response at different LGG-m^6Ascore levels in the CGGA patients. Infiltration levels of Mϕs in different m^6Ascore group in TCGA cohort (H) and CGGA cohort (I). (J) Different expressed genes between mouse bone marrow-derived Mϕs treated with IL-6 and control group. (K) GSEA results of GO (biological process) gene sets between mouse bone marrow-derived Mϕs treated with IL-6 and control group, adjusted *p* value <0.05. (L) Heatmap of cd40, tnfsf4, tnfsf9, tnfsf14 and tnfsf15. (M-R) The boxplots show the expression levels of IL-6, CD40, TNFSF4, TNFSF9, TNFSF14 and TNFSF15 between high m^6Ascore groups and the other groups. The former are based on the TCGA dataset and the latter are based on the CGGA dataset. Statistical significance was corresponded to *p* values: ns>0.05, * <0.05, ** <0.01, *** <0.001.

Supplementary Files

This is a list of supplementary files associated with this preprint. Click to download.

- Supplementarytables.xlsx
- SupportingFigs.docx